JOURNAL OF AIRCRAFT
Vol. 35, No. 6, November–December 1998

Engineering Notes

ENGINEERING NOTES are short manuscripts describing new developments or important results of a preliminary nature. These Notes cannot exceed 6 manuscript pages and 3 figures; a page of text may be substituted for a figure and vice versa. After informal review by the editors, they may be published within a few months of the date of receipt. Style requirements are the same as for regular contributions (see inside back cover).

Development of an Unstructured Mesh Method

Hong-Chia Lin*
National Huwei Institute of Technology,
Huwei, Yunlin 632, Taiwan, Republic of China

I. Introduction

THIS paper describes an independent effort in developing an unstructured mesh generator and a Euler solver for fast and accurate steady-state flow simulations in three dimensions.[1]

A popular scheme for computational fluid dynamics (CFD) applications is the advancing front method,[2] which mimics the crystal growth process. Usually a background mesh is prescribed for mesh size control and the surface mesh is required to be compatible with the background meshing parameters to facilitate the volume mesh generation.

A different approach is developed here, which does not use any background meshes but still retains some control over the mesh density. It does not need the surface mesh to be compatible with any background meshing parameters; hence, the surface mesh can be generated by using any finite element preprocessor.

Two types of flow solvers, the central-difference schemes with artificial dissipations[3] and the upwind schemes, are usually used for Euler equations. Both types of schemes are coded and tested. The upwind scheme is found to require much less mesh points to obtain good accuracy and it is more robust. The explicit scheme of Frink et al.[4] is used in this work and it is made implicit by a point implicit method similar to that of Thareja et al.[5]

The NACA research wing–body configuration[6] is used to demonstrate the tetrahedral mesh generation and to test the flow solvers. A vertical fin, horizontal stabilizers, underwing pylons, stores, and flow-through engine nacelles are added to the NACA research wing–body to increase the geometrical complexity. A flow solution at Mach number 0.9 and an angle of attack of 4 deg demonstrates that this approach does work for very complex shapes.

II. Volume Mesh Generation

The advancing front method uses the surface meshes as front or fronts. The volume grid is then grown from the front surfaces. The front size gradually decreases to zero. The size and number of fronts vary during the forming process. When all fronts vanish, the volume mesh generation is finished. To obtain an $N \log N$ algorithm in generating a mesh of size N, suitable data structure for inserting, deleting, and searching the front data is very important.

Received Nov. 29, 1995; revision received March 2, 1998; accepted for publication March 4, 1998.

*Associate Professor, Department of Aeronautical Engineering, 64, Wen-Hsa Road.

Bonet and Peraire[7] propose an alternate digital tree (ADT), which is adopted by Peraire et al.[8] Löhner[9] uses both the heap-list and quadtree/octree. In this work the ADT and heap-list are employed. The ADT can add and delete elements dynamically and it stores only the elements in the fronts. After actual coding is done, it is found that a single ADT data structure is enough to store the front data.[8] The mesh size data are handled by a heap-list.

The tetrahedron generation algorithm is similar to that of Peraire et al. and some ideas from Wey and Li[10] are included to increase its robustness. It consists of the following steps.

1) Set up the boundary or boundaries. Put all front triangle data into the ADT and the size data of triangles into the heap, which pushes the smallest triangle to the top of the heap.

2) Take the first triangle in the heap as a base for the tetrahedron to be generated and remove it from the heap. If no element exists in the heap, the mesh generation is completed.

3) Find the three angles between the base and its three neighboring triangles by the ADT search routine. If they already form a tetrahedron, go to 7. If the minimum one is less then a specified angle, a new tetrahedron is formed with the associated triangles and the base, go to 7. If the minimum angle is greater than the specified one, go to 4.

4) Determine the optimum point P to be added to form a new tetrahedron. This optimum point is determined by the autostretching method described later.

5) Collect the points that are inside a sphere centered at P from the previous ADT search result and also put some helping points into a queue.

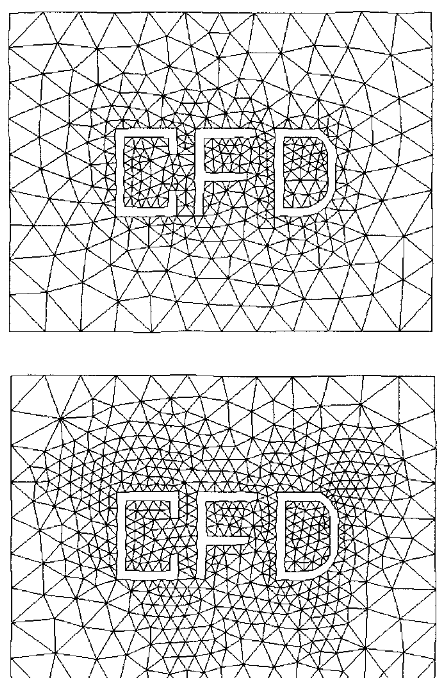

Fig. 1 Meshes for the three-character shape with SR = 1.2 and 1.1.

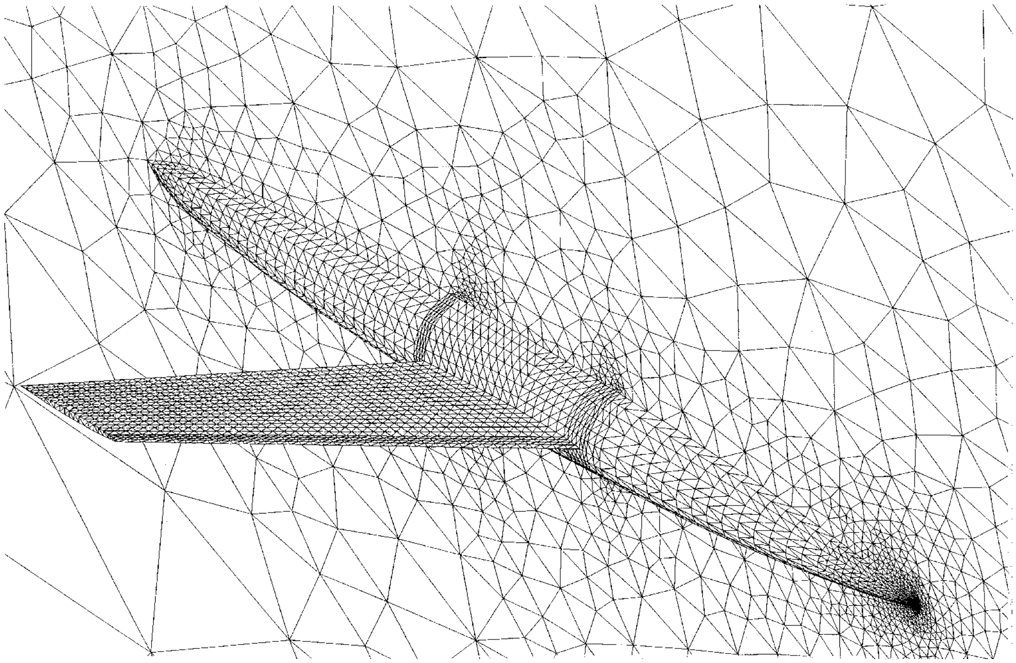

Fig. 2 Surface mesh for the research wing–body.

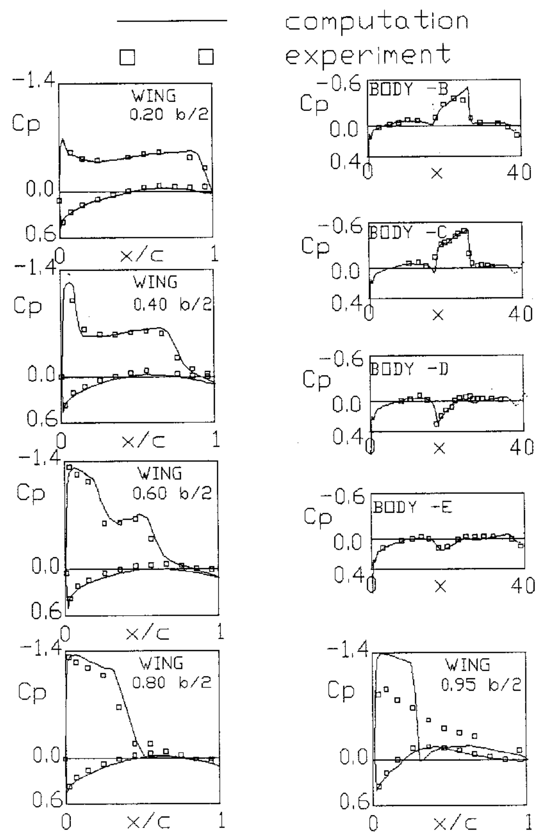

Fig. 3 Comparisons of C_p distributions on the research wing–body at $M_\infty = 0.9$ and angle of attack = 6 deg.

6) Check if the points in the queue can form a new tetrahedron with the base without intersecting with the remaining triangles in the front by using ADT search to find the possible intersection. If no intersection is found, form a tetrahedron or tetrahedra. Go to 7.

7) Delete and add new front data to ADT and heap if necessary. Go to 2.

The idea of autostretching is simple. Its success rests on the robustness of the preceding algorithm. A reference point O is chosen, which is at or near the center of the computational domain. The ideal far-field shape is a sphere, but other shapes are possible. The radius of this sphere, RFAR, and the representative length scale of the far-field triangles, SFAR, are given as input parameters. The far-field triangles are required to be of similar sizes. A fixed stretching ratio, SR, is specified for mesh stretching if the local length scale, SLOC, is less than a specified value, SFIX. If SLOC is greater than SFIX, the stretching ratio is adjusted by the following relationship

$$SR = \frac{SFAR * (RLOC + SLOC)}{SLOC * RFAR} \tag{1}$$

where RLOC is the distance between the point O and the centroid of the base triangle. The stretching ratio can be further adjusted depending on the angle between the normal of the base triangle and the vector pointed from the reference point to the centroid of the base triangle. This method can also use a reference line if slightly modified.

III. Results and Discussions

A three-character shape is used to demonstrate the autostretching method in two dimensions. The grids using two different values of SR are shown in Fig. 1.

The wing–body configuration[6] consists of a circular body of revolution with a fineness ratio 10.0 and a wing with 45-deg sweepback of the 0.25-chord line, aspect ratio 4, taper ratio 0.6, and NACA 65A006 airfoil sections. Very comprehensive pressure measurements are available. For the wing, the chordwise C_p distributions are presented at 20, 40, 60, 80, and 95% semispan stations. For the fuselage, the longitudinal pressure coefficients are given at six stations. A good test condition for Euler simulations is at Mach number 0.9 and angle of attack 6 deg. The flow features include a small outboard leading-edge vortex and a lambda shock system on the upper wing.

The surface mesh contains 3021 nodes and 5842 triangles (Fig. 2). With SR = 1.15 and SFIX = 5 in., the volume mesh has 75,015 tetrahedra and 14,941 nodes.

If the schemes with artificial dissipations are used, the leading-edge vortex cannot be captured without substantial refine-

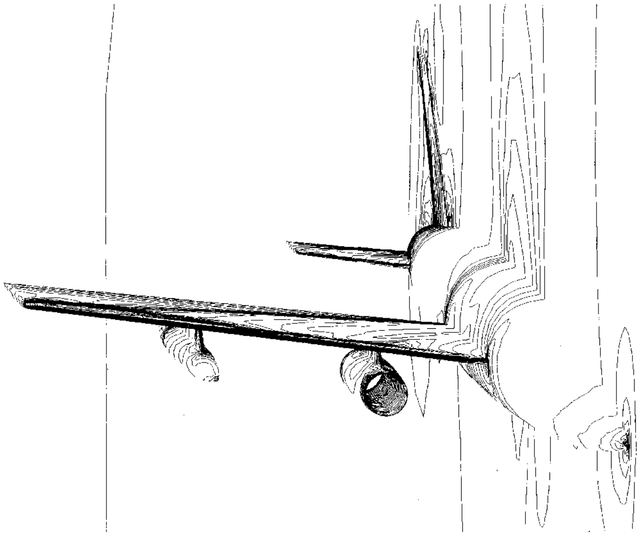

Fig. 4 C_p **contours at 0.05 intervals on the aircraft configuration at** M_∞ **= 0.9 and angle of attack = 4 deg.**

ment of this mesh. On the contrary, the upwind scheme can capture the vortex accurately. The residual is reduced by 3.5 orders of magnitude in 800 iterations. Note that this condition is also computed by using a total variation diminishing scheme in a multiblock grid with 89,012 nodes.[11] The computed results are compared with wind-tunnel results in Fig. 3. The lambda shock on the upper wing and the small leading-edge vortex are well captured. The wingtip flow is subject to strong viscous effect and cannot be resolved by using the Euler equations. Overall, the computed result is within what one would expect from a good Euler simulation.

The wing–body configuration is not complicated enough to demonstrate the autostretching method. To show this mesh generator does work, vertical and horizontal tails, pylon-mounted flow-through engine nacelles, and stores are added to the wing–body configuration without considering any aircraft design rules. To generate the volume mesh, the stretching ratio used is 1.15. A total of 119,797 tetrahedra and 23,139 nodes are generated with 4208 nodes on the surface. The flow condition is Mach number 0.9 and an angle of attack of 4 deg. The C_p contours are shown in Fig. 4. Because there is no experimental data and the mesh is not fine enough, discussion on the flowfield is therefore not attempted.

References

[1]Lin, H.-C., "An Auto-Stretching Method for Fast Generation of Unstructured Grids for Complex Configurations," *Proceedings of the 17th National Conference on Theoretical and Applied Mechanics* (Taipei, Taiwan, ROC), Chinese Society of Theoretical and Applied Mechanics, 1993, pp. 43–50.

[2]Peraire, J., Vahdati, M., Morgan, K., and Zienkiewicz, O. C., "Adaptive Remeshing for Compressible Flow Computations," *Journal of Compuational Physics*, Vol. 72, No. 4, 1987, pp. 449–466.

[3]Jameson, A., Baker, T. J., and Weatherill, N. P., "Calculation of Inviscid Transonic Flow over a Complete Aircraft," AIAA Paper 86-0103, Jan. 1986.

[4]Frink, N. T., Parikh, P., and Pirzadeh, S., "A Fast Upwind Solver for the Euler Equations on Three-Dimensional Unstructured Meshes," AIAA Paper 91-0102, Jan. 1991.

[5]Thareja, R. R., Stewart, J. R., Hassan, O., Morgan K., and Peraire, J., "A Point Implicit Unstructured Grid Solver for the Euler and Navier-Stokes Equations," *International Journal for Numerical Methods in Fluids*, Vol. 9, No. 5, 1989, pp. 405–425.

[6]Loving, D. L., and Estabrooks, B. B., "Transonic-Wing Investigation in the Langley 8-Foot High-Speed Tunnel at High Subsonic Mach Numbers and at Mach Number of 1.2—Analysis of Pressure Distribution of Wing-Fuselage Configuration Having a Wing of 45 Sweepback, Aspect Ratio 4, Taper Ratio 0.6, and NACA 65A006 Airfoil Section," NACA RM L51F07, May 1951.

[7]Bonet, J., and Peraire, J., "An Alternate Digital Tree Algorithm for Geometric Search and Intersection Problems," *International Journal for Numerical Methods in Engineering*, Vol. 31, No. 1, 1991, pp. 1–17.

[8]Peraire, J., Morgan, K., and Peiro, J., "Unstructured Mesh Methods for CFD," von Kármán Inst. for Fluid Dynamics Lecture Series 1990-06, Brussel, Belgium, 1990.

[9]Löhner, R. L., "Some Useful Data Structures for the Generation of Unstructured Grids," *Communications in Applied Numerical Methods*, Vol. 4, No. 2, 1988, pp. 123–135.

[10]Wey, T. C., and Li, C. P., "Numerical Simulation of Shuttle Ascent Transonic Flow Using an Unstructured-Grid Approach," *Computers and Structure*, Vol. 39, No. 1/2, 1991, pp. 21–46.

[11]Wang, C.-J., and Chakravarthy, S. R., "Transonic Euler Calculations of a Wing-Body Configuration Using a High-Accuracy TVD Scheme," AIAA Paper 88-2547, July 1988.

Effects of Asymmetric Leading-Edge Flap Deflection on Delta Wings in Roll

Carlos Ize* and Andrew S. Arena Jr.†
Oklahoma State University,
Stillwater, Oklahoma 74078

Introduction

A STUDY has been conducted to explore the effects of leading-edge vortex flaps on the rolling moment of delta wings over a wide angle of attack range. Leading-edge flaps with a conical planform were tested on flat plate delta wings of 65- and 80-deg sweep angles. The effects of antisymmetric deflection was investigated to assess the effectiveness of the flaps for this task over a wide operating envelope. Data are collected over a wide range of angles of attack that includes attached and separated flow conditions.

Experimental Setup

Experiments were conducted in the indraft wind tunnel at Oklahoma State University. The test section has a 0.93 × 0.93 m cross section and a length of 2.81 m. Throughout the study, a tunnel dynamic pressure of 244 Pa was maintained. The conditions were the same for all experiments.

The delta wing models used in the experiments had 65- and 80-deg sweep angles and are shown in Figs. 1a and 1b. Both were made out of aluminum, and the planform area was equal to 428 cm^2 for both wings. Each leading edge was beveled 45 deg and the flaps were such that at each chord station the flap span was 20% of the local span, yielding a conical geometry.

The torque sensor was of cruciform type, and was used to measure rolling moment C_l. The torque sensor was built to be a temperature-compensated Wheatstone bridge. The wing and the sensor were sting mounted in a base to minimize downstream interference effects, shown in Fig. 1c.

The rolling moment for the wings with flaps deflected was measured at angles of attack from $\alpha = -2$ to $+32$ deg in 2-deg increments. The flaps were set at $\delta = 25$ deg antisymmetrically, relative to the wing, with the port flap being downward and the starboard flap upward.

Received Sept. 10, 1997; revision received June 9, 1998; accepted for publication June 24, 1998.

*Graduate Research Assistant, School of Mechanical and Aerospace Engineering. Student Member AIAA.

†Assistant Professor, School of Mechanical and Aerospace Engineering. Senior Member AIAA.